Risk-averse Optimal Participation of a DR-intensive Microgrid in Competitive Clusters considering Response Fatigue

Marcos Tostado-Véliz[1], Hany M. Hasanien[2,3], Ahmad Rezaee Jordehi[4], Rania A. Turky[5], Francisco Jurado[1,*]

1. Department of Electrical Engineering, University of Jaén, 23700 Linares, Spain (e-mail: mtostado@ujaen.es (M.T.-V.), fjurado@ujaen.es (F.J.)).
2. Electrical Power and Machines Department, Faculty of Engineering, Ain Shams University, Cairo 11517, Egypt (e-mail: hanyhasanien@ieee.org).
3. Department of Electrical and Computer Engineering, Florida International University, Miami, FL 33174, USA.
4. Department of Electrical Engineering, Rasht Branch, Islamic Azad University, Rasht, Iran (e-mail: ahmadrezaeejordehi@gmail.com).
5. Electrical Engineering Department, Faculty of Engineering and Technology, Future University in Egypt, Cairo, Egypt (e-mail: Rania.turky@fue.edu.eg)

* Correspondence: fjurado@ujaen.es

Abstract. The massive integration of renewable generators, energy storage systems, and demand response requires the development of smart power infrastructures. In this upcoming context, microgrids will be essential for the optimal integration of such assets. When different microgrids are located near each other, they can be centrally coordinated within a novel paradigm called Microgrid Cluster. In such structures, the microgrids involved can collaborate in a cooperative way or compete by developing internal market structures. This paper develops a novel optimal bidding strategy for a demand response-intensive microgrid partaking in competitive clusters. The new proposal is envisaged as a three-stage methodology that aims at reducing the effects of response fatigue. Uncertainties related to inflexible demand and renewable generation are modeled via scenarios, while the risk associated with uncertain parameters is handled by enforcing the Conditional Value at Risk. The resulting computational tool is effective and tractable, as shown in the results obtained on a benchmark three-microgrids cluster. Indeed, the developed methodology is able to reduce the total response signals by 88 % in some cases. Moreover, this case study allows analyzing the effect of response fatigue minimization in the overall cluster performance, showing that the collective welfare can be reduced by 32 % when response fatigue is taken into account.

Keywords. Demand response; Microgrid cluster; Response fatigue; Risk-averse optimization; Stochastic programming.

Nomenclature

Indices (sets)	
i, j $(\mathcal{M})$	Microgrid
ω (Ω)	Scenario
t $(\mathcal{T})$	Time
Θ_i^{Def}	Allowable Time window of a deferrable consumer in the i^{th} Microgrid
Superscripts	
$Cluster$	Microgrid cluster
DG	Distributed generation
DR	Demand response
$Import/Export$	Imported/exported power
$Curt/Def/Shed$	Curtailable/deferrable/sheddable demand
RES	Renewable energy source
$BES, ch/dch$	Battery energy storage in charging/discharging mode
NC	Inflexible (non-controllable) demand
$\underline{(\cdot)}/\overline{(\cdot)}$	Minimum/maximum value of a parameter or variable
Parameters and constants	
Δt	Time step [h]
a_i^{DG}, b_i^{DG}, c_i^{DG}	Parameters of the fuel cost curve of distributed generators in the i^{th} Microgrid [\$/h, \$/kWh, \$/kWh²]
κ	Penalty cost for applying DR programs [\$/h or \$/kWh]
L_i^{Def}	Preferred earliest time step of the time window of deferrable demand in the i^{th} Microgrid
α	CVaR parameter [-]
ρ	Probability of occurrence [pu]
RD/RU	Downward/upward ramping rate [kW]
DC_i^{Def}	Duty cycle of deferrable demand in the i^{th} Microgrid
η	Efficiency [pu]
β	Risk-averse parameter [-]
π	Bidding/offering price of microgrids [\$/kWh]
M	Large positive number (~10^5) [-]
Γ	Incremental cost [-]
Decision variables	
p	Power [kW]
y	Commitment status [Binary]
on/off	ON/OFF status [Binary]
v/u	CVaR auxiliary variables [-]
SOC	State-of-charge [kWh]
$\underline{\mu}/\overline{\mu}$	Dual variable associated with lower/upper bound of imported or exported powers [-]
λ	Cluster price [\$/kWh]
ψ	Auxiliary variable for linearization of complementarity terms [Binary]

1 - Introduction

1.1 - Context and motivation

The decarbonization of the electricity sector requires the massive integration of renewable energy sources (RESs) and energy storage. In this regard, Microgrid (MG) has emerged as a valuable framework to integrate and coordinate such resources in upscale systems [1]. When different MGs are located near each other and connected to a common network, they can be centrally coordinated within a novel paradigm called MG cluster (MGC) [2]. Gathering MGs in clusters brings multiple advantages, like optimal participation in energy markets or continuous supply [3]. From a mercantilist point of view, MGCs can be cooperative or competitive. In the former case, the MGs partaking in the cluster sharing resources with others without expecting a monetary counterpart. In contrast, energy markets are launched in competitive platforms similar to conventional electricity markets [4].

This paper focuses on competitive MGCs. In particular, we discuss the optimal bidding strategy of a demand response (DR) intensive MG within clusters. It is well-known that DR, when successfully applied, helps to improve the economy and efficiency of the system [5]. However, DR initiatives must be planned and applied appropriately. Otherwise, these programs may fail. One of the main reasons for DR failure is the so-called response fatigue [6], which describes the discouragement experienced by flexible consumers when they are required to partake in DR initiatives repeatedly [7, 8]. For instance, if a curtailable consumer is frequently required to reduce her consumption, she may leave the DR program in the long-period because the dissatisfaction that multiple calling cause on herself. Due to its importance in DR implementation, the consideration of response fatigue in DR-oriented systems is worth to be investigated.

1.2 - Literature review

Most of existing works do not refer to the term MGC specifically. Instead, a number of them are referred to multi-MGs systems. Since both terms are similar and frequently used indistinctly, this review collects work referred to both MGCs and multi-MGs systems. Actually, some existing works deal with distribution networks including MGs, focusing on optimal coordination or scheduling problems. In [9], a game-based bi-level decision-making framework was developed for distribution systems in the presence of MGs. This reference contemplates the possibility of DR agreements between the distribution system operator and the MGs. A bi-level price-settling mechanism was developed in [10], focusing on distribution networks with MGs. In that framework, the distribution system operator acts as a leader, whereas MGs partake as followers within a Stackelberg-based game approach. Qiu, et al. [11] proposed a two-stage coordination framework for distribution networks and MGs, considering uncertainties in renewable generation and loads. This reference employs the column-and-constraint generation algorithm to convert the

original nonlinear problem into mixed-integer-linear programming (MILP). A stochastic-based approach was developed in [12] for optimal coordination of the distribution network operator and MGs. In this case, the problem was raised as a bi-level framework converted to a single-level scheme via mathematical programming with equilibrium constraints (MPEC). In [13], the optimal coordination between the distribution network and MGs was solved using different algorithms. In particular, column-and-constraint generation and target-cascading algorithms were applied in a decentralized manner. Likewise, [14] established an equilibrium problem with equilibrium constraints (EPEC) for optimal price-settling in a distribution network incorporating MGs. Yan, et al. [15] propose a bi-level framework with peer-to-peer (P2P) transactions among MGs. This reference concerns privacy issues, for which two distributed algorithms were proposed for power allocation among peers.

In other cases, the authors refer to the term multi-MG without specifying if the participants are integrated into an upscale system involving a central operator. To coordinate the operation of various MGs on the whole, [16] considers a central aggregator responsible for transactions among peers. To optimally operate the whole system, a bi-level optimization model was developed, considering perfect cooperation among agents. To preserve peers' privacy, [17] uses the alternating direction of multipliers on an isolated multi-MGs system. Nezamabadi and Vahidinasab [18] developed an optimal bidding strategy based on MPEC for multi-MGs systems. This reference proposes an interval-based notation for uncertainties based on three representative scenarios (favorable, unfavorable, and expected). Then, the algorithm becomes risk-averse by enforcing the conditional value-at-risk (CVaR). The coordination among MGs allows them to partake in upscale markets, where individual MGs could not be integrated effectively. This issue was contemplated in [19], where an EPEC model was established for optimal price settling of multi-MGs systems partaking in local energy and reserve markets. This reference analyzes the role of interruptible loads as a form of DR to improve the overall performance of the system.

The concept of MGC is relatively new and became to be seriously studied in the mid-2010s [20]. In essence, an MGC is a group of MGs that are coordinated centrally or in a distributed manner. Some recent works refer specifically to the term MGC, e.g. [21], where the concept of combined cooling-heating MGCs was introduced, referring to clusters where different energy vectors (i.e., electricity, heat, and cool) are encompassed and managed on the whole. In particular, [21] introduced various consensus mechanisms for the optimal coordination of MGCs. To preserve the robustness against uncertain parameters, chance-constrained models are incorporated on the basis of scenarios and seek a risk-averse solution. In [22], an MPEC-based model was developed for the optimal coordination of competitive MGCs. This reference deals with hybrid AC/DC clusters, incorporating uncertainties via robust formulation solved using the column-and-constraint generation algorithm. Xu, et al. [23] focused on optimal controlling converter-based DC MGs through droop curves. Then, the MGs involved are coordinated within a cluster structure

via scenarios. In [24], decentralized coordination of MGCs was investigated, for which a solution methodology based on the alternating direction of multipliers was employed. In this sense, the operation of the different agents is inhibited by privacy data from others. It is worth mentioning that [24] deals with multi-energy clusters, encompassing electricity, heating, and cooling sub-systems. For the sake of simplicity, Table 1 shows a summary of the studied literature.

1.3 - Research gaps and contributions

This work is motivated by various gaps encountered in the literature above. On the basis of the summary of Table 1, the following gaps are worthy of mention:

- Most of the existing works focus on the figure of the central coordinator or similar. This agent is responsible for price-settling in the cluster. However, optimal bidding strategies are frequently more useful and implementable for only one strategic MG. In this regard, only [18] focused on optimal bidding for strategic MGs.
- Although most of the relevant works present MILP formulations, some references use quadratic or nonlinear models, which are hardly solvable and often require the use of off-the-shelf solvers.
- DR programs have not been widely studied, and most of the existing works recur to only one type of DR initiative. In this sense, DR-intensive MGs have not been profusely studied yet.
- In the same line, the effect of response fatigue has only been modeled and analyzed in MGs context in [8]. However, this reference focuses on isolated MGs, ignoring interactions with other systems and how the response fatigue affects to the collective welfare and energy transactions among MGs.
- Many works ignore the impact of uncertainties recurring in simplistic deterministic problems. On the other hand, other references recur to stochastic programming but without including a risk measurement indicator that accounts for the overall impact of uncertainties. Finally, other works raised complex two-stage or bi-level frameworks that may be hardly implementable.

Table 1 - A summary of the relevant literature

Ref.	Problem	Formulation	Model	DR	Uncertainty model	Response fatigue
[9]	Price-settling	MILP	Bi-level with a single leader and multiple followers	Load shifting	No	No
[10]	Price-settling	MILP	Bi-level Stackelberg-based clearing mechanism	Shiftable demand	Two-stage robust	No
[11]	Optimal scheduling	MILP	Two-stage robust model using column-and-constraint generation	No	Two-stage robust	No
[12]	Price-settling	MILP	Bi-level MPEC model with a single leader and multiple followers	Sheddable loads	Stochastic	No
[13]	Economic dispatch	MILP	Bi-level MPEC model solved using cascading target and column-and-constraint algorithms	No	Robust	No
[14]	Price-settling	MILP	Bi-level EPEC approach solved using diagonalization	Curtailable loads	No	No
[15]	Price-settling	MILP + privacy preserved heuristic	Distributed optimization model based on optimal behavior of buyers and sellers	Curtailable demand	No	No
[16]	Price-settling	Nonlinear	MPEC with multiple followers and a single leader	No	No	No
[17]	Market participation	Quadratic	Bi-level model solved using alternating direction method of multipliers	No	No	No
[18]	Optimal bidding	MILP	Bi-level MPEC focused on only one strategic MG	Curtailable demand	Equivalent scenarios (CVaR)	No
[19]	Market participation	MILP	EPEC formulation	Interruptible loads	No	No
[21]	Price-settling	MILP	Consensus-based coordinated solution	No	Chance-constrained	No
[22]	Price-settling	Quadratic	Bi-level model solved using column-and-constraint generation algorithm	No	Robust	No
[23]	Price-settling	Quadratic	Bi-level MPEC solved using the alternating direction of multipliers	No	Stochastic	No
[24]	Price-settling	Quadratic	Decentralized framework based on the alternating direction of multipliers	No	Stochastic	No
Present	Optimal bidding	MILP	Bi-level MPEC + developed solution algorithm	• Curtailable loads • Sheddable loads • Deferrable loads	Risk-averse stochastic (CVaR)	Yes

To fill the gaps commented above, this paper contributes with some important points to the existing literature. Maybe the two major contributions are: firstly, developing an optimal bidding for DR-intensive MGs for partaking in MGCs; secondly, incorporating and analyzing the effect on DR fatigue on the operation of this kind of MGs and its effect on the overall cluster performance. In this regard, this paper presents important improvements over other existing works. For instance, [8] considers minimizing the effect of response fatigue on optimal operation of MGs. However, this reference focuses on isolated MGs and therefore their interactions with other agents are ignored. On the other hand, [18] developed an optimal bidding strategy for MGs in clusters. Nevertheless, the effect of response fatigue was ignored and only curtailable demand

was modelled, neglecting the flexibility provided by other kind of DR initiatives. Moreover, we develop an original three-stage solution methodology which can be considered an original contribution. Indeed, this methodology serves to solve bi-objective optimization problems by simply exchanging information among stages. In this regard, this procedure supposes a contribution in the field of multi-objective optimization together with other well-known methodologies like weighting functions and Lexicographic optimization. For simplicity, the main contributions of this paper are listed below:

i. Developing a risk-averse optimal bidding strategy for DR-intensive MGs partaking in MGCs. The problem is formulated as a bi-level framework, which is converted to a single-level problem (MPEC) and further linearized to be totally MILP, being so easily solvable by conventional solvers.
ii. Uncertainties are modeled via scenarios, and a scenario-reduction methodology is proposed. Then, the problem becomes risk-averse by enforcing the CVaR term in the objective function. This way, risk associated to uncertainties is properly managed using a simple approach, in contrast to other more complicated models like interval notation.
iii. In contrast to most of the existing works that only focused on one DR model, this paper considers different DR initiatives (curtailable, deferrable and sheddable loads) which are specifically modeled and introduced in the problem. Their impact on final performance is analyzed.
iv. The effect of response fatigue is included in the model. To do that, DR signals are modeled and a three-stage solution procedure is developed to minimize the effect of response fatigue while the economy of the system is maximized on a whole.

In the rest of this paper, Section 2 describes the problem and the uncertainty modeling. Section 3 presents the mathematical formulation for the optimal bidding strategy proposed. Section 4 models the DR signals. Section 5 develops a multi-stage algorithm for response fatigue minimization. Section 6 presents and comments on various numerical results. The paper is concluded with Section 7.

2 - Preliminaries

2.1 - System model

This paper focuses on an MGC such as that outlined in Fig. 1. The cluster is formed by n MGs, which are individually operated by MG operators. There exists a cluster operator who is responsible for determining the cluster price and scheduling energy transactions among peers. This way, the MGs submit their bidding/offer prices (π), and the cluster operator performs a price-settling mechanism to establish the final prices in the cluster (λ) in order to maximize the collective welfare.

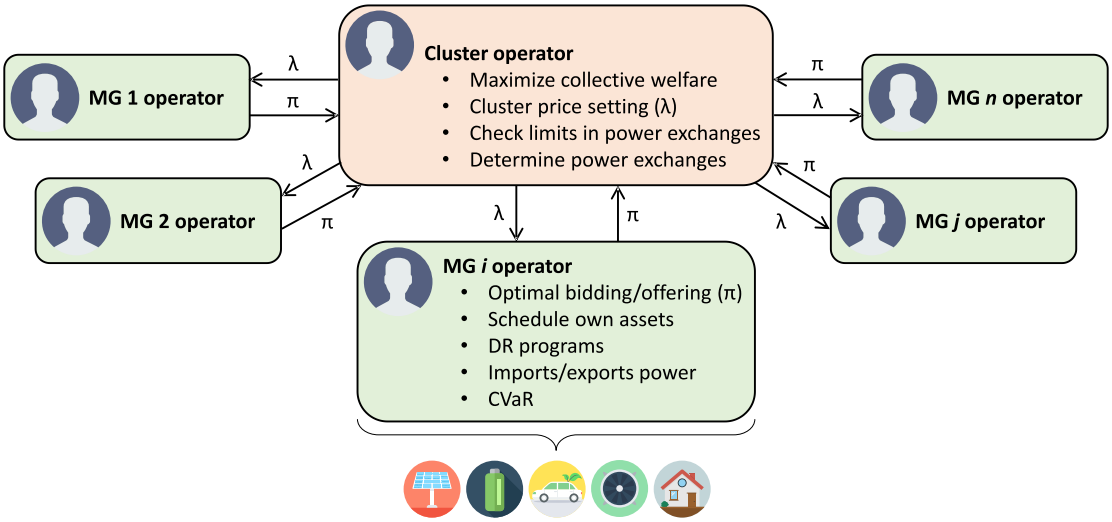

Fig. 1 - Scheme of the considered MGC structure

It is assumed that each MG counts with own assets. However, this work focuses on the optimal bidding strategy of the i^{th} MG partaking in the cluster. Thus, this MG can schedule distributed generators (DGs), renewable units, and battery energy storage (BES). Moreover, this MG can import or export energy from other peers in the cluster under the established price λ. Moreover, it is assumed that the i^{th} MG in the cluster is DR-intensive, i.e., it is focused on optimally exploiting flexible consumers to improve its monetary results. In particular, three different DR programs are considered [25]:

- Curtailable demand: these consumers can adjust their consumption within predefined bounds. They are compensated for each kWh curtailed.
- Sheddable demand: these consumers can be disconnected from the network for convenience, and, in consequence, they are disabled to import energy from the MG. They are compensated for each hour disconnected. In this regard, we assume that these consumers agree with the operator the possibility of being disconnected, passing this responsibility to this agent. Therefore, although they voluntary agree the participation in sheddable programs, they are disconnected from the system under the operator's decision.
- Deferrable demand: these consumers can defer their consumption within predefined time windows. Nevertheless, they must complete a preestablished duty cycle. This way, these consumers are similar to the controllable appliances in home energy management problems [26]. These consumers are compensated for each hour their operation is advanced/delayed.

2.2 - Uncertainty modelling

Essentially, the MG operation is affected by uncertainties in renewable generation and non-controllable demand. To deal with these uncertain parameters, probabilistic or robust methodologies can be adopted. Each approach has pros and cons; nevertheless, if probability

distributions of uncertain parameters are known and available, probabilistic methodologies are widely preferred because their simplicity and adaptability. In this sense, both uncertainties (i.e. renewable generation and non-controllable demand, are normally considered predictable and subjected to low random patterns [26, 27]. This way, we adopt a scenario-based representation of such uncertainties. In this regard, we assume that both renewable generation and demand can be day-ahead predicted with acceptable accuracy. However, conventional forecast techniques are subjected to errors and therefore predicted profiles are not 100 % accurate. Typically, it is assumed that forecast errors can be modelled following a well-established probability distribution. In this work, we assume that forecast errors follow Gaussian distribution [28], which is a feasible assumption since the expected profiles, although not exact, are more probable than large errors. Based on this distribution, around 1000 scenarios are generated to represent the deviation of uncertain parameters from their expected values. Since this number of scenarios is hardly tractable in practice (note that decision variables present the same dimension as the number of scenarios generated), a scenario-reduction methodology is proposed in this paper. The proposed methodology is based on the k-medoids method, which generally shows good features [29]. This clustering technique is based on the traveller problem and reduces the original scenario space to a minimum set of representative profiles called medoids. In practice, these medoids are assumed to be a good representation of the entire scenario space. The k-medoids method presents a degree of freedom, i.e., the total number of clusters (representative scenarios). Fixing this number heuristically is difficult since it should be sufficiently high to accurately represent the original scenarios but low yet to keep the model tractable. To select this number, we propose to use a combination of the elbow method and triangle threshold. This methodology is sketched in Fig. 2, and its main steps are given below:

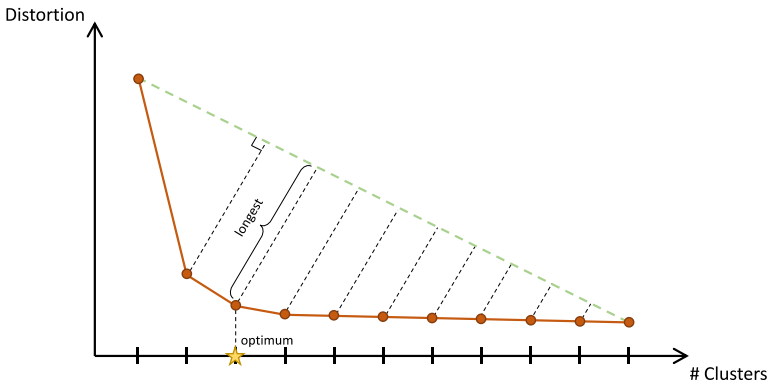

Fig. 2 - Sketch of the proposed methodology for cluster number selection

1. Perform the k-medoids method for only one cluster to a sufficiently large number of clusters (~50).
2. Calculate the distortion (i.e. the total sum of distances of all the data with respect to their corresponding medoids [27]) for each cluster number (orange line in Fig. 2).

3. Draw a line that crosses the extreme points in the distortion line (green discontinuous line in Fig. 2).
4. Draw an orthogonal line from the line drawn in Step 3 and each point of the distortion curve.
5. The longest line is associated with the optimum and therefore represents the ideal number of clusters.
6. Calculate the probability of occurrence of each cluster as explained in [26].

It is worth noting that both uncertain profiles (i.e. renewable generation and non-controllable demand) can be gathered in the same matrix notation to serve as common inputs to the proposed clustering model. It can be done since the number of generated scenarios is high, thus eliminating possible interdependences between parameters.

3 - Optimal bidding strategy of a DR-intensive MG

This section presents the mathematical model referred to the optimal bidding strategy for a DR-intensive MG partaking in an MGC. The model is developed as a bi-level framework, which is further converted to a single-level problem (MPEC) and finally linearized (MILP) to be easily tractable.

3.1 - MG operational model

The MG operational cost encompasses the cost of exchanging energy in the cluster, fuel costs, and compensatory payments to flexible consumers, as follows:

$$Cost_{i,\omega,t} = \Delta t \cdot \left(C_{i,\omega,t}^{Cluster} + C_{i,\omega,t}^{DG} + C_{i,\omega,t}^{DR}\right) \quad (1)$$

In (1), the first term stands for the cost of energy exchanging with the cluster, which is calculated as a function of the cluster price, as follows:

$$C_{i,\omega,t}^{Cluster} = \lambda_{\omega,t}^{Cluster} \cdot \left(p_{i,\omega,t}^{Import} - p_{i,\omega,t}^{Export}\right); \forall \omega \in \Omega \wedge t \in \mathcal{T} \quad (2)$$

The second and third terms in (1) represent the fuel cost of DGs and expenditures for applying DR programs, respectively. These two terms are developed in (3) and (4). As seen, the fuel cost is calculated as a quadratic function of the energy generated [25], while DR payments respond to the premises explained in Section 2.1.

$$C_{i,\omega,t}^{DG} = y_{i,t}^{DG} \cdot a_i^{DG} + p_{i,\omega,t}^{DG} \cdot b_i^{DG} + \left(p_{i,\omega,t}^{DG}\right)^2 \cdot c_i^{DG}; \forall \omega \in \Omega \wedge t \in \mathcal{T} \quad (3)$$

$$C_{i,\omega,t}^{DR} = \kappa_i^{Curt} \cdot \left(\overline{p}_{i,t}^{Curt} - p_{i,\omega,t}^{Curt}\right) + \kappa_i^{Shed} \cdot \left(|\mathcal{T}| - y_{i,t}^{Shed}\right) + \kappa_i^{Def} \cdot \left| \begin{bmatrix} \mathrm{on}_{i,1}^{Def} \\ \vdots \\ \mathrm{on}_{i,|\mathcal{T}|}^{Def} \end{bmatrix}^T \cdot \begin{bmatrix} 1 \\ \vdots \\ |\mathcal{T}| \end{bmatrix} - \mathrm{L}_i^{Def} \right|; \forall \omega \in \Omega \wedge t \in \mathcal{T} \quad (4)$$

It is worth noting that (3) can be easily linearized using piecewise representations [25], whereas the absolute value in (4) can be further linearized using the big-M method as described in [26].

To measure the risk against uncertainties, we consider a well-established chance-constrained measurement. Chance-constrained programming problems ensure that the probability of occurrence of some constrains is kept beyond a predefined threshold. In practice, these constraints do not have a closed-form expression and are, in general, non-convex. To overcome such issues, the Value-at-Risk (VaR) can be used to linearize the model [30]. However, CVaR is normally preferred as it approximates the value of the Value-at-Risk keeping the model convex [31]. In this regard, (5) represents the CVaR term, which considers the risk associated with uncertainty. In (5), $\alpha \in [0,1]$ is the so-called CVaR parameter, which means that the $\alpha - \text{CVaR}$ is the average of the expected monetary loss for potential loss values that exceed the $\alpha - \text{VaR}$ threshold. In this paper, $\alpha = 0.9$ is taken, whereas (6) and (7) complete the CVaR model [32].

$$\text{CVaR}_t(\alpha) = v_t + \frac{1}{1-\alpha} \cdot \sum_{\forall \omega} \rho_\omega \cdot u_{\omega,t}\,; \forall t \in \mathcal{T} \tag{5}$$

$$Cost_{i,\omega,t} - v_t \leq u_{\omega,t}; \forall \omega \in \Omega \wedge t \in \mathcal{T} \tag{6}$$

$$u_{\omega,t} \geq 0; \forall \omega \in \Omega \wedge t \in \mathcal{T} \tag{7}$$

In subsequent headings, we describe the components modelling involved in MG operation.

Power balance

The power balance in the MG is ensured by imposing (8), which takes into account the flexibility provided by DR, while (9) ensures that simultaneous imports and exports are avoided (note that $\perp$ stands for complementarity, which is equivalent to $p_{i,\omega,t}^{Import} \cdot p_{i,\omega,t}^{Export} = 0$).

$$p_{i,\omega,t}^{Import} + p_{i,\omega,t}^{DG} + p_{i,\omega,t}^{RES} + p_{i,\omega,t}^{BES,dch} = p_{i,\omega,t}^{Export} + p_{i,\omega,t}^{NC} + p_{i,\omega,t}^{Curt} + y_{i,t}^{Shed} \cdot \overline{p}_{i,t}^{Shed} + y_{i,t}^{Def} \cdot \overline{p}^{Def} + p_{i,\omega,t}^{BES,ch}; \forall \omega \in \Omega \wedge t \in \mathcal{T} \tag{8}$$

$$0 \leq p_{i,\omega,t}^{Import} \perp p_{i,\omega,t}^{Export} \geq 0; \forall \omega \in \Omega \wedge t \in \mathcal{T} \tag{9}$$

It is worth commenting that since the non-controllable demand is inhibited from any scheduling plan and only responds to unpredictable human decisions, the parameter $p_{i,\omega,t}^{NC}$ is considered uncertain and modelled using input scenarios, as described in Section 2.2.

DG modelling

DGs are modelled by upper and lower bounds in power generation (10) and ramping limits in (11).

$$y_{i,t}^{DG} \cdot \underline{p}^{DG} \leq p_{i,\omega,t}^{DG} \leq y_{i,t}^{DG} \cdot \overline{p}^{DG}; \forall \omega \in \Omega \wedge t \in \mathcal{T} \tag{10}$$

$$p_{i,\omega,t-1}^{DG} - RD_i^{DG} \leq p_{i,\omega,t}^{DG} \leq p_{i,\omega,t-1}^{DG} + RU_i^{DG}; \forall \omega \in \Omega \wedge t \in \mathcal{T} \backslash t = 1 \tag{11}$$

RES modelling

Eq. (12) ensures that renewable generation does not surpass the predicted potential power. This potential generation is considered unknown and treated as an uncertain parameter, as explained in Section 2.2.

$$p_{i,\omega,t}^{RES} \leq \overline{p}_{i,\omega,t}^{RES}; \forall \omega \in \Omega \wedge t \in \mathcal{T} \quad (12)$$

Curtailable demand modelling

Curtailable loads can adapt their consumption within bounds for convenience. Therefore, the dispatched curtailable power must be properly limited, as said (13).

$$\underline{p}_{i,t}^{Curt} \leq p_{i,\omega,t}^{Curt} \leq \overline{p}_{i,t}^{Curt}; \forall \omega \in \Omega \wedge t \in \mathcal{T} \quad (13)$$

Deferrable demand modelling

Deferrable loads can be scheduled within preestablished time windows. In any case, they must complete their duty cycles within time windows, as said (14), while (15) and (16) impose continuous operation.

$$\sum_{t \in \Theta_i^{Def}} y_{i,t}^{Def} = \mathrm{DC}_i^{Def} \quad (14)$$

$$y_{i,t}^{Def} - y_{i,t-1}^{Def} = \mathrm{on}_{i,t}^{Def} - \mathrm{off}_{i,t}^{Def}; \forall \omega \in \Omega \wedge t \in \mathcal{T} \backslash t = 1 \quad (15)$$

$$\sum_{\forall t} \mathrm{on}_{i,t}^{Def} = 1 \quad (16)$$

BES modelling

State-of-charge (SOC) is calculated by (17) as a function of the SOC in the previous step and power exchanged. On the other hand, SOC must be limited by the nominal capacity of batteries and depth-of-discharge settings, as said (18). The maximum power that batteries can exchange with the system is upper limited to rated values by (19), whereas (20) ensures that charging and discharging processes are complementary. Lastly, since (17) is not defined at the beginning of the time horizon, the BES initial SOC is given by (21). To keep the model coherent, this same constraint ensures that the initial and final SOC are the same.

$$SOC_{i,\omega,t}^{BES} = SOC_{i,\omega,t-1}^{BES} + \Delta t \cdot \left(p_{i,\omega,t}^{BES,ch} \cdot \eta_i^{BES,ch} - \frac{p_{i,\omega,t}^{BES,dch}}{\eta_i^{BES,dch}} \right); \forall \omega \in \Omega \wedge t \in \mathcal{T} \backslash t = 1 \quad (17)$$

$$\underline{SOC}_i^{BES} \leq SOC_{i,\omega,t}^{BES} \leq \overline{SOC}_i^{BES}; \forall \omega \in \Omega \wedge t \in \mathcal{T} \quad (18)$$

$$p_{i,\omega,t}^{BES,x} \leq \overline{p}_i^{BES}; \forall \omega \in \Omega \wedge t \in \mathcal{T} \wedge x \in \{ch, dch\} \quad (19)$$

$$0 \leq p_{i,\omega,t}^{BES,ch} \perp p_{i,\omega,t}^{BES,dch} \geq 0; \forall \omega \in \Omega \wedge t \in \mathcal{T} \quad (20)$$

$$SOC_{i,\omega,1}^{BES} = SOC_{i,\omega,|\mathcal{T}|}^{BES} = \overline{SOC}_i^{BES}; \forall \omega \in \Omega \quad (21)$$

Integrity constraints

The MG operational model is completed by imposing integrity in binary constraints with (22).

$$y_{i,t}^{DG}, y_{i,t}^{Shed}, y_{i,t}^{Def}, \mathrm{on}_{i,t}^{Shift}, \mathrm{off}_{i,t}^{Shift} \in \{0,1\}; \forall t \in \mathcal{T} \quad (22)$$

3.2 - MG optimal bidding - upper level

The MG optimal bidding problem is formulated as a bi-level optimization framework. In the upper level, the MG operational cost is minimized, considering the risk associated with uncertainty through CVaR. At this level, the bidding strategy of the i^{th} MG is decided according to the following optimization problem:

$$\begin{cases} \min\limits_{\Xi_i^{MG} \cup \pi_{i,\omega,t}} \sum_{\forall t}\left\{(1-\beta)\cdot\sum_{\forall \omega}\left\{\rho_\omega \cdot Cost_{i,\omega,t}\right\} + \beta \cdot \mathrm{CVaR}_t(\alpha)\right\} \\ \text{subject to: } (6)-(22) \\ \pi_{i,\omega,t} \geq 0; \forall \omega \in \Omega \wedge t \in \mathcal{T} \end{cases} \tag{23}$$

where Ξ_i^{MG} stands for the vector of decision variables of the i^{th} MG operational model, and β is the risk-aversion factor [32], which measures the degree of robustness of the problem. Indeed, if $\beta = 0$, the problem adopts a risk-neutral strategy, while the optimization procedure becomes more conservative as the value of β grows.

3.3 - MG optimal bidding - lower level

In the lower level, the cluster price $\lambda_{\omega,t}^{Cluster}$ is settled in order to maximize the collective welfare, which can be calculated as follows [33]:

$$WF_{\omega,t} = \Delta t \cdot \sum_{\forall j} \pi_{j,\omega,t} \cdot \left(p_{j,\omega,t}^{Import} - p_{j,\omega,t}^{Export}\right); \forall \omega \in \Omega \wedge t \in \mathcal{T} \tag{24}$$

In the lower level, the power exchanged among MGs is bounded by either contractual or physical limits in (25), while (26) ensures the power balance in the cluster.

$$0 \leq p_{j,\omega,t}^{x} \leq \overline{p}_{j,t} : \underline{\mu}_{j,\omega,t}^{x}, \overline{\mu}_{j,\omega,t}^{x}; \forall j \in \mathcal{M} \wedge \omega \in \Omega \wedge t \in \mathcal{T} \wedge x \in \{Import, Export\} \tag{25}$$

$$\sum_{\forall j} p_{j,\omega,t}^{Import} = \sum_{\forall j} p_{j,\omega,t}^{Export} : \lambda_{\omega,t}^{Cluster}; \forall \omega \in \Omega \wedge t \in \mathcal{T} \tag{26}$$

It is worth noting that dual variables associated with constraints (25) and (26) are shown on the right-hand side of their respective equations. Finally, the lower level of the presented optimal bidding strategy is stated in (27).

$$\begin{cases} \max\limits_{\Xi_{primal}^{Cluster}} \sum_{\forall t}\left\{\sum_{\forall \omega}\left\{\rho_\omega \cdot WF_{\omega,t}\right\}\right\} \\ \text{subject to: } (25), (26) \end{cases} \tag{27}$$

where $\Xi_{primal}^{Cluster}$ stands for the vector of primal variables of the lower level problem.

3.4 - MG optimal bidding - MPEC reformulation

The optimal bidding problem described above is stated as a bi-level framework. This kind of problems are NP-hard and normally require the use of off-the-shelf solvers, which make them difficult to solve. However, due to the lower level is linear, it can be passed to the upper level using its Karush-Kuhn-Tucker (KKT) conditions [33], thus describing a MPEC model. In this regard, (28) and (29) represent the stationary conditions of the lower level, while (30) stands for the complementarity conditions. Lastly, (31) imposes positivity in the dual variables μ [18].

$$-\pi_{j,\omega,t} - \underline{\mu}_{j,\omega,t}^{Import} + \overline{\mu}_{j,\omega,t}^{Import} + \lambda_{\omega,t}^{Cluster} = 0; \forall j \in \mathcal{M} \wedge \omega \in \Omega \wedge t \in \mathcal{T} \tag{28}$$

$$\pi_{j,\omega,t} - \underline{\mu}_{j,\omega,t}^{Export} + \overline{\mu}_{j,\omega,t}^{Export} - \lambda_{\omega,t}^{Cluster} = 0; \forall j \in \mathcal{M} \wedge \omega \in \Omega \wedge t \in \mathcal{T} \tag{29}$$

$$0 \leq \begin{matrix} \overline{\mu}_{j,\omega,t}^{x} \perp \left(\overline{p}_{j,t} - p_{j,\omega,t}^{x}\right) \\ \underline{\mu}_{j,\omega,t}^{x} \perp p_{j,\omega,t}^{x} \end{matrix} \geq 0; \forall j \in \mathcal{M} \wedge \omega \in \Omega \wedge t \in \mathcal{T} \wedge x \in \{Import, Export\} \tag{30}$$

$$\underline{\mu}_{j,\omega,t}^{x}, \overline{\mu}_{j,\omega,t}^{x} \geq 0; \forall j \in \mathcal{M} \wedge \omega \in \Omega \wedge t \in \mathcal{T} \wedge x \in \{Import, Export\} \tag{31}$$

Incorporating the constraints (28)-(31), the lower level can be integrated into the upper level, thus forming a single-level structure as follows:

$$\begin{cases} \min\limits_{\substack{\Xi_i^{MG} \cup \pi_{i,\omega,t} \cup \\ \Xi_{primal}^{Cluster} \cup \Xi_{dual}^{Cluster}}} \sum_{\forall t}\left\{(1-\beta) \cdot \sum_{\forall \omega}\left\{\rho_\omega \cdot Cost_{i,\omega,t}\right\} + \beta \cdot \mathrm{CVaR}_t(\alpha)\right\} \\ \text{subject to: } (6)-(22), (25), (26), (28)-(31) \\ \pi_{i,\omega,t} \geq 0; \forall \omega \in \Omega \wedge t \in \mathcal{T} \end{cases} \tag{32}$$

where $\Xi_{dual}^{Cluster}$ stands for the vector of dual variables of the lower level problem.

3.5 - MG optimal bidding - MILP reformulation

The MPEC model (32) is nonlinear due to 1) complementarity constraints (9), (20), and (30), and 2) bi-linear terms in the objective function. To linearize the complementarity terms, we use the big-M method, as follows [33]:

$$0 \leq \delta_{v_1} \perp \delta_{v_2} \geq 0 \equiv \begin{cases} \delta_{v_1} \geq 0, \delta_{v_2} \geq 0 \\ \delta_{v_1} \leq M \cdot \psi_v \\ \delta_{v_1} \leq M \cdot (1-\psi_v) \\ \psi_v \in \{0,1\} \end{cases}; \forall v \in \{(9), (20), (30)\} \tag{33}$$

While the strong-duality theorem [34] is used to linearize (1) as follows:

$$\tilde{C}_{i,\omega,t}^{Cluster} = \sum_{\forall j \neq i}\left\{\pi_{j,\omega,t} \cdot \left(p_{j,\omega,t}^{Import} - p_{j,\omega,t}^{Export}\right) - \overline{p}_{j,t} \cdot \left(\overline{\mu}_{j,\omega,t}^{Import} + \overline{\mu}_{j,\omega,t}^{Export}\right)\right\} \tag{34}$$

$$\widetilde{Cost}_{i,\omega,t} = \Delta t \cdot \left(C_{i,\omega,t}^{DG} + C_{i,\omega,t}^{DR} - \tilde{C}_{i,\omega,t}^{Cluster}\right) \tag{35}$$

With the linearization tricks above, the MPEC model (32) is transformed into the MILP single-level optimization problem (36), easily solvable by off-the-shelf solvers.

$$\begin{cases} \min\limits_{\substack{\Xi_i^{MG} \cup \pi_{i,\omega,t} \cup \Psi \cup \\ \Xi_{primal}^{Cluster} \cup \Xi_{dual}^{Cluster}}} \sum_{\forall t}\left\{(1-\beta) \cdot \sum_{\forall \omega}\left\{\rho_\omega \cdot \widetilde{Cost}_{\omega,t}\right\} + \beta \cdot \mathrm{CVaR}_t(\alpha)\right\} \\ \text{subject to: } (6)-(22), (25), (26), (28)-(31), (33) \\ \pi_{i,\omega,t} \geq 0; \forall \omega \in \Omega \wedge t \in \mathcal{T} \end{cases} \tag{36}$$

where Ψ is the vector of the ψ's auxiliary variables.

4 - Modelling DR signals

To consider the effect of response fatigue in our model, DR signals have to be properly modelled. We understand that any flexible consumer receives a DR signal when she is required to modify her predefined consumption pattern. This way, the total DR signals received by sheddable consumers are easily modellable, as follows:

$$\Upsilon_i^{Shed} = |\mathcal{T}| - \sum_{\forall t} y_{i,t}^{Shed} \tag{37}$$

Indeed, as (37) said, sheddable consumers receive as many DR signals as hours are required to be disconnected from the MG. On the other hand, curtailable consumers receive DR signals when they are required to adjust their consumption. To model these signals, we introduce the virtual commitment status $y_{i,t}^{Curt}$, which responds to the following model:

$$y_{i,t}^{Curt} = \begin{cases} 1, \text{if } \overline{p}_{i,t}^{Curt} > p_{i,\omega,t}^{Curt} \\ 0, \text{o.w.} \end{cases}; \forall \omega \in \Omega \wedge t \in \mathcal{T} \tag{38}$$

As observed in (38), $y_{i,t}^{Curt}$ effectively represents the DR signals received by curtailable consumers as this variable is equal to 1 when the dispatched power is lower than the predefined power profile. However, constraint (38) represents a logical rule that cannot be directly integrated into MILP frameworks. To solve this, we use the big-M method, as follows [25]:

$$\begin{cases} M \cdot y_{i,t}^{Curt} \geq \overline{p}_{i,t}^{Curt} - p_{i,\omega,t}^{Curt} \\ M \cdot \left(1 - y_{i,t}^{Curt}\right) \geq p_{i,\omega,t}^{Curt} - \overline{p}_{i,t}^{Curt} \end{cases}; \forall \omega \in \Omega \wedge t \in \mathcal{T} \tag{39}$$

Thus, making use of (39), the total DR signals received by curtailable consumers can be calculated as follows:

$$\Upsilon_i^{Curt} = \sum_{\forall t} y_{i,t}^{Curt} \tag{40}$$

Lastly, we assume that deferrable consumers are keen to be scheduled at the beginning of her preferred time windows [26]. Nevertheless, they could be yet scheduled within allowable time slots. Therefore, they receive as many DR signals as hours are advanced/delayed in their preferred timetable. Keeping this in mind, the total DR signals received by deferrable consumers can be calculated as follows:

$$\Upsilon_i^{Def} = \left| \begin{bmatrix} \mathrm{on}_{i,1}^{Def} \\ \vdots \\ \mathrm{on}_{i,|\mathcal{T}|}^{Def} \end{bmatrix}^T \cdot \begin{bmatrix} 1 \\ \vdots \\ |\mathcal{T}| \end{bmatrix} - \mathrm{L}_i^{Def} \right| \tag{41}$$

With the models established above, the total DR signals are calculated by (42) and minimized using the Lexicographic procedure (43).

$$\Upsilon_i = \Delta t \cdot \left(\Upsilon_i^{Shed} + \Upsilon_i^{Curt} + \Upsilon_i^{Def}\right) \tag{42}$$

$$\begin{cases} \min\limits_{\Xi_i^{MG}} \Upsilon_i \\ \text{subject to: } (6) - (22), (39) \\ \sum_{\forall t} \sum_{\forall \omega} \rho_\omega \cdot \left(\tilde{C}_{i,\omega,t}^{Cluster} + C_{i,\omega,t}^{DG}\right) \leq (1 + \Gamma) \cdot \underline{Cost}^{Cluster+DG} \end{cases} \tag{43}$$

where Γ is the so-called incremental cost, which represents the per-unit margin available to increment the costs with the objective of reducing the response fatigue. In other words, it is evident that response fatigue is minimized at the expenses of incrementing the operational MG cost. However, it is assumed that operators are not willing to increment their costs beyond a limit given by Γ (see [8] for further details). In (43), $\underline{Cost}^{Cluster+DG}$ represents a lower bound for the cost of exchanging energy in the cluster and DG fuel consumption. How to calculate this bound is explained in the following section.

5 - The developed solution procedure

Actually, the problem raised in this paper is a bi-objective optimization framework. Indeed, the developed procedure aims at improving the economy of the studied MG while response fatigue is minimized. Addressing this problem with a single-stage methodology is complicated as both objectives must be incorporated in the same objective function using, for example, weighting operators. This methodology, although simple, entails multiple issues [26]. Alternatively, we propose a three-stage framework in which each objective is optimized separately, but the information exchanged among stages makes possible to reach a compromise solution between objectives. The main steps of the developed procedure are outlined in the flowchart of Fig. 3 and detailed in the following sub-sections.

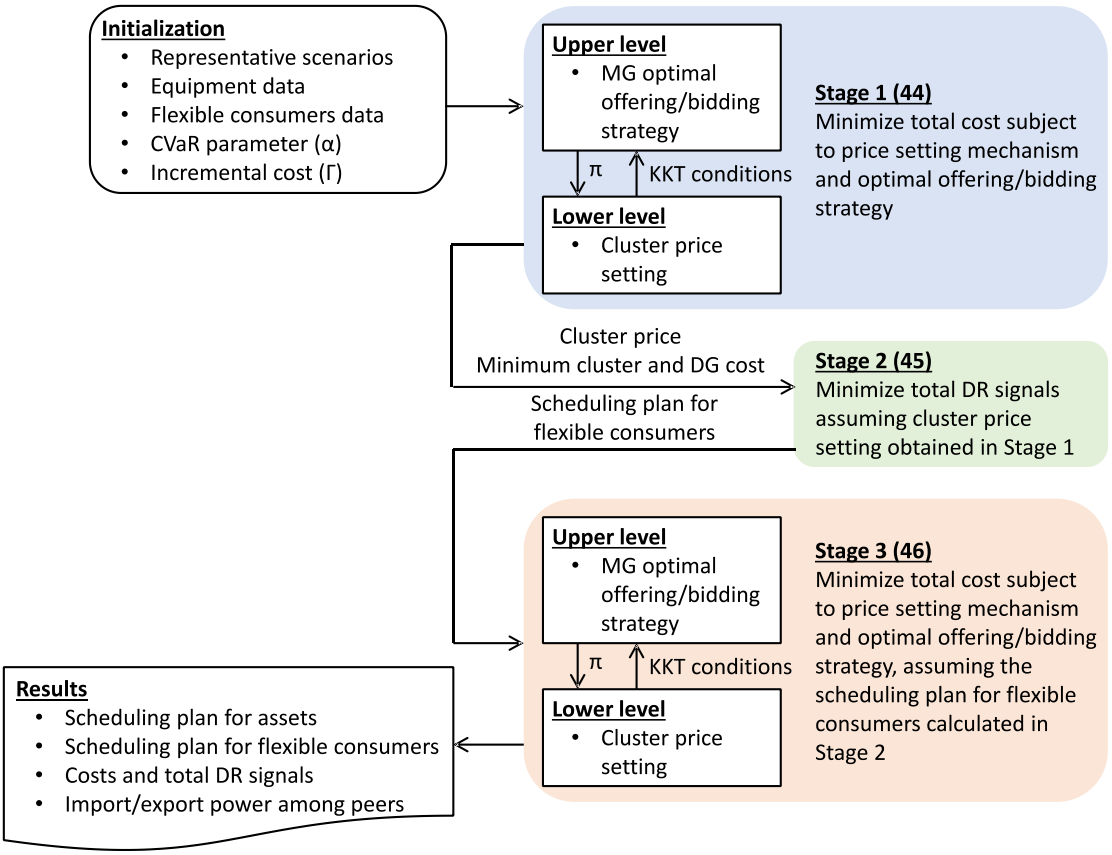

Fig. 3 - Flowchart of the developed solution procedure

5.1 - Stage 1 - Price-settling without considering response fatigue

At stage 1, the cluster operator settles the cluster price, and the bidding strategy for the considered MG is decided without considering response fatigue. Hence, this stage corresponds with the resolution of the two-level bidding problem described in Section 3, as follows:

$$\begin{cases} \tilde{\lambda}_{\omega,t}^{Cluster}; \\ \forall \omega \in \Omega \wedge t \in \mathcal{T} \end{cases} \rightarrow \underset{\substack{\Xi_i^{MG} \cup \pi_{i,\omega,t} \cup \Psi \cup \\ \Xi_{primal}^{Cluster} \cup \Xi_{dual}^{Cluster}}}{\operatorname{argmin}} \sum_{\forall t} \begin{Bmatrix} (1-\beta) \cdot \sum_{\forall \omega} \{\rho_\omega \cdot \widetilde{Cost}_{\omega,t}\} \\ +\beta \cdot \mathrm{CVaR}_t(\alpha) \end{Bmatrix}$$
$$\begin{cases} \text{subject to: } (6)-(22), (25), (26), (28)-(31), (33) \\ \pi_{i,\omega,t} \geq 0; \forall \omega \in \Omega \wedge t \in \mathcal{T} \\ \underline{Cost}^{Cluster+DG} = \sum_{\forall t} \sum_{\forall \omega} \rho_\omega \cdot \left(\tilde{C}_{i,\omega,t}^{Cluster} + C_{i,\omega,t}^{DG}\right) \end{cases} \quad (44)$$

As observed, the problem (44) does not take care of response fatigue. Thereby, the system is only optimized from an economic point of view, no matter how many times the flexible consumers are called to partake in the system operation.

As a result of this stage, we obtain a first approximation of the cluster price $\tilde{\lambda}_{\omega,t}^{Cluster}$. Moreover, as the MG operational cost is the unique objective to be minimized, the lower bound for the fuel and energy exchanging expenditures can also be calculated. These two values serve as inputs for the second stage.

5.2 - Stage 2 - Minimizing response fatigue via Lexicographic

Taking the estimated cluster price and minimum cost obtained at the first stage, the second stage aims at minimizing the response fatigue, as follows:

$$\begin{cases} \tilde{y}_{i,t}^{Shed}, \tilde{y}_{i,t}^{Curt}, \tilde{y}_{i,t}^{Def}; \\ \forall t \in \mathcal{T} \end{cases} \rightarrow \underset{\Xi_i^{MG}}{\operatorname{argmin}}\, \Upsilon_i$$
$$\begin{cases} \text{subject to: } (6)-(22), (39) \\ \sum_{\forall t} \sum_{\forall \omega} \rho_\omega \cdot \left(\tilde{C}_{i,\omega,t}^{Cluster}\left(\tilde{\lambda}_{\omega,t}^{Cluster}\right) + C_{i,\omega,t}^{DG}\right) \leq (1+\Gamma) \cdot \underline{Cost}^{Cluster+DG} \end{cases} \quad (45)$$

As previously commented, this stage minimizes the response fatigue at the expense of incrementing the fuel and energy trading expenditures, representing Γ the allowable incremental margin. As a result of this stage, one obtains the scheduling plan for DR loads (the $\tilde{y}$'s) that minimizes response fatigue.

5.3 - Stage 3 - Price-settling considering response fatigue

Finally, response fatigue is incorporated into the price-settling mechanism. To do that, the DR scheduling plan obtained at stage 2 is taken fixed at this stage. This way, one ensures that response fatigue is kept at its minimum. Under this established schedule, the price-settling problem is performed again with the object of yielding the overall scheduling plan for MG assets and energy exchanging that minimizes the MG operational cost, as follows:

$$\begin{cases} \underset{\substack{\Xi_i^{MG} \cup \pi_{i,\omega,t} \cup \Psi \cup \\ \Xi_{primal}^{Cluster} \cup \Xi_{dual}^{Cluster}}}{\min} \sum_{\forall t} \left\{(1-\beta) \cdot \sum_{\forall \omega} \left\{\rho_\omega \cdot \widetilde{Cost}_{\omega,t}\right\} + \beta \cdot \mathrm{CVaR}_t(\alpha)\right\} \\ \text{subject to: } (6)-(22), (25), (26), (28)-(31), (33), (39) \\ \pi_{i,\omega,t} \geq 0; \forall \omega \in \Omega \wedge t \in \mathcal{T} \\ y_{i,t}^{Shed} = \tilde{y}_{i,t}^{Shed}, y_{i,t}^{Curt} = \tilde{y}_{i,t}^{Curt}, y_{i,t}^{Def} = \tilde{y}_{i,t}^{Def}; \forall t \in \mathcal{T} \end{cases} \quad (46)$$

6 - Results

Various numerical results are presented and commented in this section. The objective of this section is, therefore, twofold. On the one hand, we aim at validating the novel proposal, showing that the results obtained with the new tool are coherent and its computational burden does not suppose a barrier to its implantation in industry tools. On the other hand, we analyze the impact of the incremental cost (Γ) and risk-aversion factor (β) on response fatigue minimization. Various simulations were performed on a benchmark MGC whose relevant data are reported in the following section. The developed solution procedure was coded under Matlab R2021a and run on an Intel® Core™ i7-10700K CPU @ 3.80GHz with 32.00 GB RAM, using Gurobi [35] for solving the different optimization problems involved.

6.1 - Data

The simulations were performed over a 24-h time horizon with 1-h resolution ($\Delta\tau = 1$). As commented throughout this paper, non-controllable demand and renewable generation are considered uncertain parameters and therefore modelled using scenarios. According to the procedure described in Section 2.2, expected profiles of such uncertainties must be provided, which are shown in Fig. 4. Potential renewable generation was constructed using real data of solar irradiance and temperature in Madrid (Spain), on May 3, 2016 [36], assuming a 900-kW total PV capacity installed and the PV panel model described in [37]. On the other hand, the non-controllable demand was adapted from real consumption in La Palma Island (Spain) on May 3, 2016 [38]. Based on such profiles, 1000 scenarios for forecast errors were generated assuming Gaussian distributions, which were reduced to 11 representative profiles following the procedure described in Section 2.2.

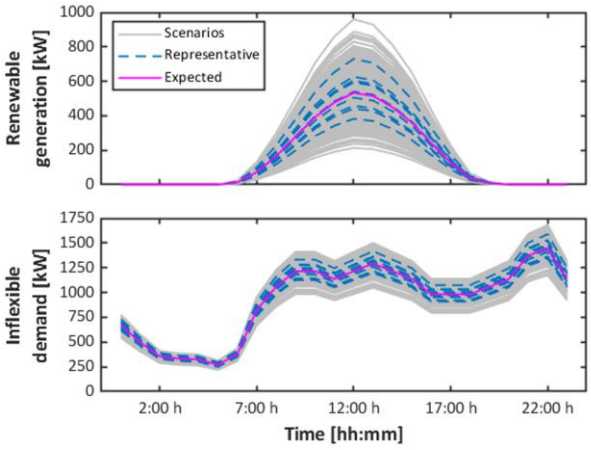

Fig. 4 - Scenarios used in simulations

Fig. 5 plots the expected demand of curtailable and sheddable consumers. The compensatory payments for each DR program are reported in Table 2 [25]. Regarding the deferrable demand, we considered a 400-kW total demand with a 7-h duty cycle and schedulable from 1:00 h to 21:00 h, establishing the preferred time period since 4:00 h. Fig. 5 also plots the expected bidding prices of rival MGs. In this case, we considered a simple 3-MG cluster in order to facilitate the analysis

of results. As seen in Fig. 5, offering price of MG2 is normally higher, except during central hours, when assuming large renewable penetration in MG2 being therefore able to exchange energy at low prices. Finally, the power exchanged among MGs is limited to 2 MW, and data regarding DGs and BES are reported in Table 3.

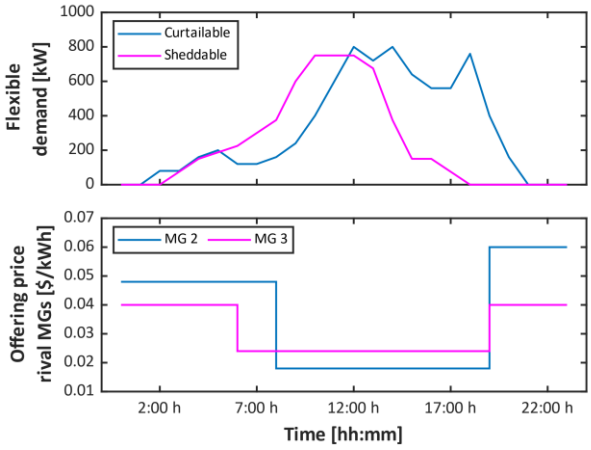

Fig. 5 - Expected demand of flexible consumers (upper) and bid prices of rival MGs (bottom)

Table 2 - Compensatory payments for DR programs

Type of DR	**Payment**
Curtailable	0.05 $/kWh
Sheddable	30 $/h
Deferrable	0.3 $/h

Table 3 - Data of DGs and BES [8]

Parameter	**Value**
DG max/min power	2000/20 kW
DG ramping rate	750 kW
a^{DG},b^{DG},c^{DG}	0.6 $/h, 0.05 $/kWh, 0.02 $/kWh²
BES capacity	500 kWh
BES power rate	250 kW
BES efficiency	98 %
BES depth-of-discharge	60 %

6.2 - Influence of the incremental cost (Γ)

Firstly, we analyze how the incremental cost (Γ) affects to the response fatigue minimization. To do that, we fix $\beta = 1$ and vary the value of Γ. This way, the optimization procedure is only focused on minimizing the costs (the CVaR term in the objective function is ignored), analyzing later the effect of the risk-aversion factor. Fig. 6 shows the total DR signals received by flexible consumers for various incremental costs (ranging from 0 to 0.1 since the total DR signals were zero beyond this value). This figure reports the total DR signals at the different stages involved in the developed procedure. As expected, the results obtained at stage 1 entail higher response fatigue. Actually, since the incremental cost is not relevant at this stage, the flexible consumers were called 17 times regardless of the value of Γ. When running stages 2 and 3, the number of DR signals was notably reduced to 7 with $\Gamma = 0$ and 2 with $\Gamma = 0.1$ These results put on manifest

two important conclusions. Firstly, the developed methodology is able to effectively reduce the effect of response fatigue. Secondly, the number of DR signals is reduced with Γ, which is a logical sense since, as Γ increases, the operator has more flexibility and flexible consumers can be scheduled attending to their own preferences and not to the overall cost.

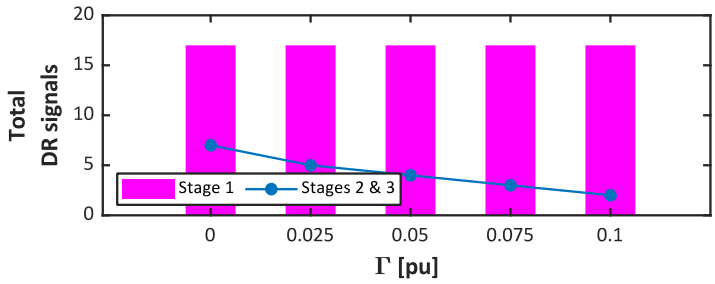

Fig. 6 - Total DR signals for various Γ and $\beta = 1$

Reduction of DR signals affects the associated DR costs (compensatory payments for applying DR programs), as shown in Fig. 7 for various values of Γ. As observed, total DR costs were reduced from ~210 $ to ~60 $ when the incremental cost increases from 0 to 0.1. This result was expected and deduced from the results in Fig. 6 since less compensations have to be paid to flexible consumers if their participation is less required. However, the collective welfare was also reduced by 32 % (~900 $), as also observed in Fig. 7. To better understand this result, let us analyze the results in Fig. 8, where the total imported/exported energy in the cluster is reported. As observed in this figure, as the value of the incremental cost grows, the energy imported by MG1 increased by 12 %, while it is reduced in the case of MG3 by 30 %. This is due to flexible consumption is less exploited as Γ increases, as was already commented in Fig. 6. It provokes that more energy must be purchased from the cluster to satisfy the demand in order to reduce the effects of response fatigue. In contrast, the total exported energy was barely affected by the value of Γ. Due to the variation of the imported energy in the MGs 1 and 3, the value of the collective welfare was reduced with the incremental cost.

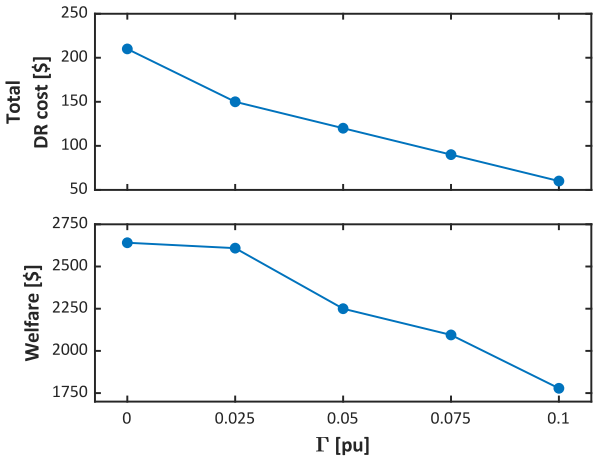

Fig. 7 - Total DR costs (upper) and collective welfare (bottom) for various Γ and $\beta = 1$

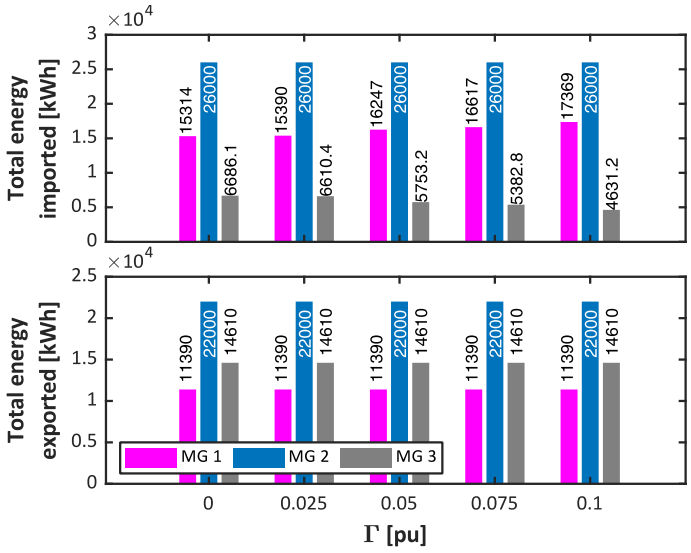

Fig. 8 - Total energy imported (upper) and exported (bottom) for various Γ and $\beta = 1$

6.3 - Influence of the risk-aversion factor (β)

To analyze the effect of the risk-aversion factor, it is taken variable while $\Gamma = 0$. This way, the effect of the incremental cost is neglected. Fig. 9 is an analogue to Fig. 6 but varying β. As seen, the effect of β is contrary to the incremental cost. Indeed, the total DR signals incremented from 17 to 26 at stage 1 and from 7 to 15 at stage 2 when incrementing the risk aversion factor from 0 to 1. This is due to, as β increases, the developed methodology becomes more risk-averse. It provokes that pessimistic scenarios are taken into consideration assuming pessimistic profiles of uncertainties. In the face of this situation, the MG under study required a more frequent participation of flexible consumers in order to keep the costs within acceptable margins. From these results, it can be concluded that the risk-aversion character of the scheduling principle has a negative effect on response fatigue, incrementing it notably.

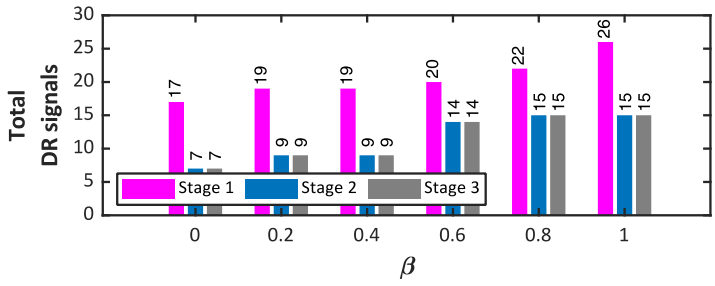

Fig. 9 - Total DR signals for various β and $\Gamma = 0$

To show how the risk-aversion factor affects the MG operational principle, Fig. 10 plots the scheduling result obtained with two extreme values of β. As seen in this figure, MG1 exported energy during dawn and evening, when the cluster price was high, and imported power during midday, when the cluster price fell. Regarding the behavior of flexible consumers, it is evident that both sheddable and curtailable demands are more frequently called when $\beta = 1$. Actually, the sheddable demand was disconnected during midday in both cases, but also in the period 4:00-

5:00 h when $\beta = 1$. In the case of the curtailable demand, it is clear that less power was dispatched in the case of $\beta = 1$ (7560 kWh vs. 6300 kWh, thus covering 84 % of the total curtailable demand with $\beta = 1$). With these results, the sheddable loads received 9 signals while the curtailable consumers were called 4 times. In this figure, it is also evident the effect of the risk-aversion factor in renewable generation. As appreciated, generation from renewables was notably lower (-14 %) in the case of $\beta = 1$ (3700 kWh vs. 3200 kWh). Thereby, the MG is operated under more pessimistic assumptions and the scheduling result becomes more robust, but at the expense of incrementing the effects of response fatigue. Lastly, Fig. 11 is an analogue to Fig. 8 but varying β. In this case, both exported and imported energy seem few affected by the value of β. Just scarce variations (~8 %) without following a clear trend. This is due to, as the risk aversion factor increases, the total renewable generation was reduced, but the flexible consumers were more frequently called at once. So that the negative effect caused by a lower renewable potential is compensated by the flexibility provided by DR initiatives, reducing the necessity of exchanging energy with other MGs.

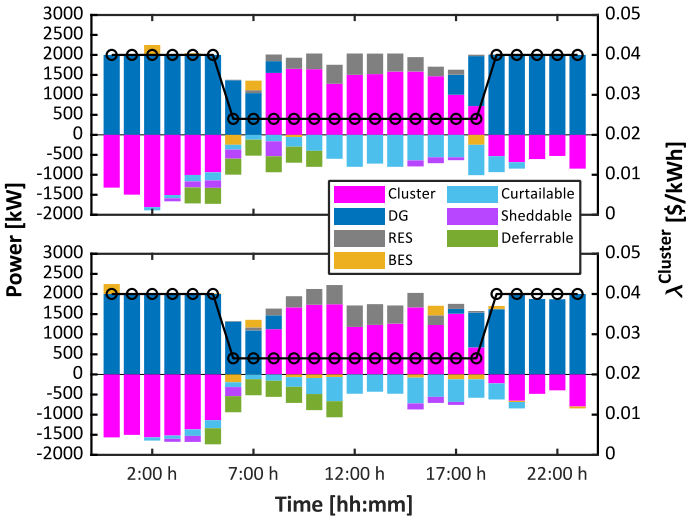

Fig. 10 - Scheduling result with Γ, $\beta = 0$ (upper), and $\beta = 1$ (bottom). In this figure, positive powers indicate to-the-MG (generation) flows whereas the black line represents the resulting cluster price (right y-axis)

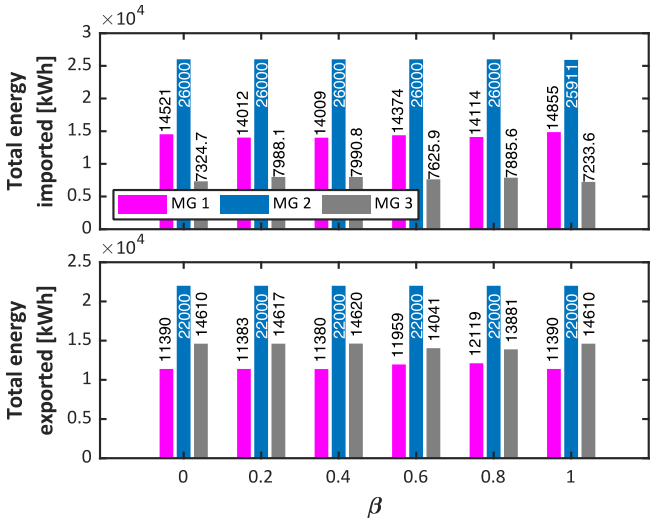

Fig. 11 - Total energy imported (upper) and exported (bottom) for various β and $\Gamma = 0$

6.4 - Joint effect of incremental cost and risk-aversion factor

To analyze what factor (Γ or β) affects more notably response fatigue, we analyze the joint effect of both parameters in Fig. 12. From this figure, it is clear that β had a more notable effect on the DR signals, especially for $\beta \geq 0.6$. This is due to the risk aversion factor tends to consider more pessimistic scenarios for renewable generation, as previously analyzed. In the face of this situation, the MG operator requires the operation of flexible consumers more frequently in order to maintain the monetary balance within allowable bounds. As previously explained and clearly evidenced in Fig. 12, the effect of both factors is opposite since while the total DR signals decrease with the value of Γ, the opposite trend is observed for β.

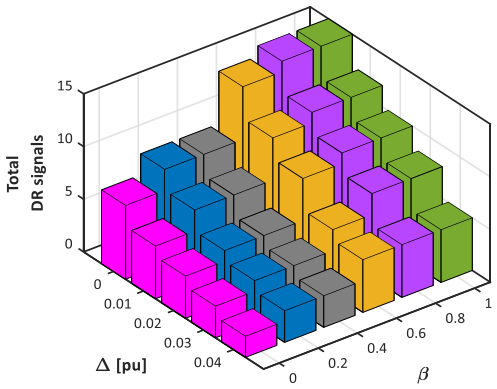

Fig. 12 - Analysis of the total DR signals for various Γ and β

6.5 - Computational efficiency analysis

Computational efficiency is a critical feature of any computational tool. Actually, the computational burden should be low enough to demonstrate the practicability and implantation of the new proposal. To this end, we carried out a computational efficiency analysis, for which, Fig. 13 shows the average time of various simulations performed for different system sizes

(number of MGs). In this case, as numerical results are not relevant, the data regarding MGs were taken arbitrary. As seen in Fig. 13, computational time attributed to stage 2 remained constant regardless of the number of MGs involved, which is coherent since, at this stage, only the concerned MG is modelled. In contrast, computational time consumed by stages 1 and 3 grew exponentially with the number of MGs partaking in the cluster. This is due to some variables in these stages have dimension $|\mathcal{M}|$. It means that the problem size increases with the number of MGs. It is worth observing that the computational time of stage 3 is always lighter than stage 1 since, at the third stage, the commitment statuses of flexible consumers are fixed while they are declared variables at stage 1. Lastly, it is worth observing that the total time consumed by the new proposal is low and reasonable for day-ahead scheduling tools, keeping it in approximately 2 hours even for large-scale systems.

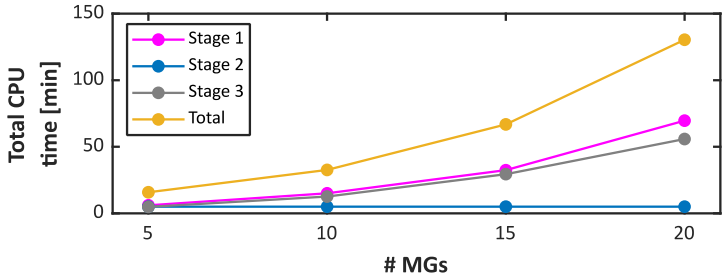

Fig. 13 - Total computational time for various system sizes

7 - Conclusions

A novel optimal bidding strategy for DR-intensive MGs partaking in MGCs has been developed. The new proposal consists of a three-stage methodology by which the optimal bid strategy is decided taking into account the effects of response fatigue. To this end, three different DR initiatives have been modelled and integrated into the model, resulting in an effective but computationally light procedure. Uncertainties related to inflexible demand and renewable generation have been modelled via scenarios, while the risk associated with such uncertainties is adaptively controlled by enforcing the CVaR through the risk-aversion factor (β).

To validate the developed methodology as well as analyze the effect of response fatigue, we performed extensive simulations on a three-MGs cluster. Among others, the results obtained allow us to extract the following conclusions:

- The incremental cost affects positively to the response fatigue, in contrast to the risk aversion factor.
- The impact of the risk-aversion factor in response fatigue is more notable than the incremental cost.
- The minimization of the response fatigue affects the overall performance of the cluster. Actually, the total welfare was reduced by 18 % when the incremental cost increased from 0 to 0.1.

Due to the good results obtained with the developed methodology, we aim at testing it in other similar problems. For instance, similar procedures can be applied to reduce the waiting time in charging infrastructures or improve the thermal comfort of residential communities. These topics will be studied in future works.

References

[1] M. McCullough. *Downtime on the Microgrid - Architecture, Electricity, and Smart City Islands*. Cambridge, MA: The MIT Press; 2020. https://doi.org/10.7551/mitpress/11953.001.0001.

[2] D.G. Rosero, N.L. Díaz, C.L. Trujillo. Cloud and machine learning experiments applied to the energy management in a microgrid cluster. *Applied Energy* 2021; 304: 117770. https://doi.org/10.1016/j.apenergy.2021.117770.

[3] F. Bandeiras, E. Pinheiro, M. Gomes, P. Coelho, J. Fernandes. Review of the cooperation and operation of microgrid clusters. *Renewable and Sustainable Energy Reviews* 2020; 133: 110311. https://doi.org/10.1016/j.rser.2020.110311.

[4] S.E. Ahmadi, N. Rezaei. An IGDT-based robust optimization model for optimal operational planning of cooperative microgrid clusters: A normal boundary intersection multi-objective approach. *International Journal of Electrical Power & Energy Systems* 2021; 127: 106634. https://doi.org/10.1016/j.ijepes.2020.106634.

[5] J.S. Vardakas, N. Zorba, C.V. Verikoukis. A Survey on Demand Response Programs in Smart Grids: Pricing Methods and Optimization Algorithms. *IEEE Communications Surveys & Tutorials* 2015; 17(1): 152-78. https://doi.org/10.1109/COMST.2014.2341586.

[6] J.-H. Kim, A. Shcherbakova. Common failures of demand response. *Energy* 2011; 36(2): 873-80. https://doi.org/10.1016/j.energy.2010.12.027.

[7] M. Shafie-Khah, P. Siano. A Stochastic Home Energy Management System Considering Satisfaction Cost and Response Fatigue. *IEEE Transactions on Industrial Informatics* 2018; 14(2): 629-38. https://doi.org/10.1109/TII.2017.2728803.

[8] M. Tostado-Véliz, S. Kamel, H.M. Hasanien, R.A. Turky, F. Jurado. Uncertainty-aware day-ahead scheduling of microgrids considering response fatigue: An IGDT approach. *Applied Energy* 2022; 310: 118611. https://doi.org/10.1016/j.apenergy.2022.118611.

[9] M. Jalali, K. Zare, H. Seyedi. Strategic decision-making of distribution network operator with multi-microgrids considering demand response program. *Energy* 2017; 141: 1059-71. https://doi.org/10.1016/j.energy.2017.09.145.

[10] Y. Liu, L. Guo, C. Wang. A robust operation-based scheduling optimization for smart distribution networks with multi-microgrids. *Applied Energy* 2018; 228: 130-40. https://doi.org/10.1016/j.apenergy.2018.04.087.

[11] H. Qiu, B. Zhao, W. Gu, R. Bo. Bi-Level Two-Stage Robust Optimal Scheduling for AC/DC Hybrid Multi-Microgrids. *IEEE Transactions on Smart Grid* 2018; 9(5): 5455-66. https://doi.org/10.1109/TSG.2018.2806973.

[12] A. N. Toutounchi, S. Seyedshenava, J. Contreras, A. Akbarimajd. A Stochastic Bilevel Model to Manage Active Distribution Networks With Multi-Microgrids. *IEEE Systems Journal* 2019; 13(4): 4190-9. https://doi.org/10.1109/JSYST.2018.2890062.

[13] X. Zhou, Q. Ai, M. Yousif. Two kinds of decentralized robust economic dispatch framework combined distribution network and multi-microgrids. *Applied Energy* 2019; 253: 113588. https://doi.org/10.1016/j.apenergy.2019.113588.

[14] A. Naebi, S.S. Shenava, J. Contreras, C. Ruiz, A. Akbarimajd. EPEC approach for finding optimal day-ahead bidding strategy equilibria of multi-microgrids in active distribution networks. *International Journal of Electrical Power & Energy Systems* 2020; 117: 105702. https://doi.org/10.1016/j.ijepes.2019.105702.

[15] M. Yan, M. Shahidehpour, A. Paaso, L. Zhang, A. Alabdulwahab, A. Abusorrah. Distribution Network-Constrained Optimization of Peer-to-Peer Transactive Energy Trading Among Multi-Microgrids. *IEEE Transactions on Smart Grid* 2021; 12(2): 1033-47. https://doi.org/10.1109/TSG.2020.3032889.

[16] F. Khavari, A. Badri, A. Zangeneh. Energy management in multi-microgrids via an aggregator to override point of common coupling congestion. *IET Generation, Transmission & Distribution* 2019; 13(5): 634-42. https://doi.org/10.1049/iet-gtd.2018.5922.

[17] Y. Zhang, Q. Ai, H. Wang, Z. Li, K. Huang. Bi-level distributed day-ahead schedule for islanded multi-microgrids in a carbon trading market. *Electric Power Systems Research* 2020; 186: 106412. https://doi.org/10.1016/j.epsr.2020.106412.

[18] H. Nezamabadi, V. Vahidinasab. Arbitrage Strategy of Renewable-Based Microgrids via Peer-to-Peer Energy-Trading. *IEEE Transactions on Sustainable Energy* 2021; 12(2): 1372-82. https://doi.org/10.1109/TSTE.2020.3045216.

[19] P. Sheikhahmadi, S. Bahramara, A. Mazza, G. Chicco, M. Shafie-Khah, J.P.S. Catalão. Multi-Microgrids Operation With Interruptible Loads in Local Energy and Reserve Markets. *IEEE Systems Journal* 2022; Early access. https://doi.org/10.1109/JSYST.2022.3177637.

[20] H. Lin, C. Liu, J.M. Guerrero, J.C. Vasquez, T. Dragicevic. Modular Power Architectures for Microgrid Clusters. In *2014 International Conference on Green Energy* 2014; Sfax, Tunisia: 199-206. https://doi.org/10.1109/ICGE.2014.6835422.

[21] X. Zhou, Q. Ai. Distributed economic and environmental dispatch in two kinds of CCHP microgrid clusters. *International Journal of Electrical Power & Energy Systems* 2019; 112: 109-26. https://doi.org/10.1016/j.ijepes.2019.04.045.

[22] Y. Fu, Z. Zhang, Z. Li and Y. Mi. Energy Management for Hybrid AC/DC Distribution System With Microgrid Clusters Using Non-Cooperative Game Theory and Robust Optimization. *IEEE Transactions on Smart Grid* 2020; 11(2): 1510-25. https://doi.org/10.1109/TSG.2019.2939586.

[23] Q. Xu, Y. Xu, Z. Xu, L. Xie, F. Blaabjerg. A Hierarchically Coordinated Operation and Control Scheme for DC Microgrid Clusters Under Uncertainty. *IEEE Transactions on Sustainable Energy* 2021; 12(1): 273-83. https://doi.org/10.1109/TSTE.2020.2991096.

[24] J. Guo et al. Decentralized Incentive-based multi-energy trading mechanism for CCHP-based MG cluster. *International Journal of Electrical Power & Energy Systems* 2021; 133: 107138. https://doi.org/10.1016/j.ijepes.2021.107138.

[25] M. Tostado-Véliz, S. Kamel, H.M. Hasanien, R.A. Turky, F. Jurado. A mixed-integer-linear-logical programming interval-based model for optimal scheduling of isolated microgrids with green hydrogen-based storage considering demand response. *Journal of Energy Storage* 2022; 48: 104028. https://doi.org/10.1016/j.est.2022.104028.

[26] M. Tostado-Véliz, S. Gurung, F. Jurado. Efficient solution of many-objective Home Energy Management systems. *International Journal of Electrical Power & Energy Systems* 2022; 136: 107666. https://doi.org/10.1016/j.ijepes.2021.107666.

[27] M. Tostado-Véliz, S. Kamel, H.M. Hasanien, P. Arévalo, R.A. Turky, F. Jurado. A stochastic-interval model for optimal scheduling of PV-assisted multi-mode charging stations. *Energy* 2022; 253: 124219. https://doi.org/10.1016/j.energy.2022.124219.

[28] M.M. Lakouraj, H. Niaz, J.J. Liu, P. Siano, A. Anvari-Moghaddam. Optimal risk-constrained stochastic scheduling of microgrids with hydrogen vehicles in real-time and day-ahead markets. *Journal of Cleaner Production* 2021; 318: 128452. https://doi.org/10.1016/j.jclepro.2021.128452.

[29] E.S. Pinto, L.M. Serra, A. Lázaro. Evaluation of methods to select representative days for the optimization of polygeneration systems. *Renewable Energy* 2020; 151: 488-502. https://doi.org/10.1016/j.renene.2019.11.048.

[30] H. Chen, Y. Kong, G. Li, L. Bai. Conditional value-at-risk-based optimal spinning reserve for wind integrated power system. *International Transactions on Electrical Energy Systems* 2016; 26(8): 1799-809. https://doi.org/10.1002/etep.2180.

[31] Y. Cao, W. Wei, S. Mei, M. Shafie-khah, J.P.S. Catalão. Analyzing and Quantifying the Intrinsic Distributional Robustness of CVaR Reformulation for Chance-Constrained Stochastic Programs. *IEEE Transactions on Power Systems* 2020; 35(6): 4908-11. https://doi.org/10.1109/TPWRS.2020.3021285.

[32] M. Tofighi-Milani, S. Fattaheian-Dehkordi, M. Gholami, M. Fotuhi-Firuzabad, M. Lehtonen. A Novel Distributed Paradigm for Energy Scheduling of Islanded Multiagent Microgrids. *IEEE Access* 2022; 10: 83636-49. https://doi.org/10.1109/ACCESS.2022.3197160.

[33] L. Baringo, M. Freire, R. García-Bertrand, M. Rahimiyan. Offering strategy of a price-maker virtual power plant in energy and reserve markets. *Sustainable Energy, Grids and Networks* 2021; 28: 100558. https://doi.org/10.1016/j.segan.2021.100558.

[34] X. Wang et al. Tri-Level Scheduling Model Considering Residential Demand Flexibility of Aggregated HVACs and EVs Under Distribution LMP. *IEEE Transactions on Smart Grid* 2021; 12(5): 3990-4002. https://doi.org/10.1109/TSG.2021.3075386.

[35] Gurobi Optimization L.L.C. Gurobi Optimizer Reference Manual, 2021. Online, available at: https://www.gurobi.com, accessed Jan. 18, 2023.

[36] European Comission. Photovoltaic Geographical Information System. Online, available at: https://re.jrc.ec.europa.eu/pvg_tools/en/tools.html, accessed Jan. 18, 2023.
[37] A. Mobasseri, M. Tostado-Véliz, A.A. Ghadimi, M.R. Miveh, F. Jurado. Multi-energy microgrid optimal operation with integrated power to gas technology considering uncertainties. *Journal of Cleaner Production* 2022; 333: 130174. https://doi.org/10.1016/j.jclepro.2021.130174.
[38] Red Eléctrica de España. 2021 Canary electricity demand in real-time. Online available at: https://www.ree.es/en/activities/canary-islands-electricity-system/canary-electricity-demand-in-real-time, accessed Jan. 18, 2023.